Methodology for Parameter Calculation of VP-GMAW

A straightforward procedure is presented for the calculation of welding parameters to reach both arc and metal transfer stability

BY L. O. VILARINHO, A. S. NASCIMENTO, D. B. FERNANDES, AND C. A. M. MOTA

ABSTRACT

The development of electronic power sources has allowed the study of innovative processes, generally with the objective to improve productivity allied to low levels of heat input. The existing processes are based on metal transfer evaluation and the development of different waveforms for improving the process control. The variable polarity gas metal arc welding (VP-GMAW) process is a derivative process of conventional GMAW that joins the advantages of the use of positive polarity, as the good stability of arc and cathodic cleaning, with the supplied ones for the negative polarity, which is the high melting rate of the electrode and low heat input to the base metal. However, this process still has a limited use due to shortage of technical and scientific literature devoted to parameter calculation, as the one observed for DC pulsed GMAW (Refs. 1, 2). Also, most of literature is dedicated to aluminum welding (Refs. 3–7). Thus, in this work, a methodology for determination of the process parameters is proposed and evaluated for different waveforms and variable electrode negative ratio (percentage of time at negative polarity). Both arc and metal transfer stabilities are observed as indicators. The experimental procedure was carried out with bead-on-plate welding of mild steel and employing high-speed filming and analysis of bead geometrical features. It is concluded that the proposed methodology is suitable for parameters calculation during VP-GMAW, where a positive base time after the negative one is more effective in reducing abrupt polarity changes and therefore provides more stable arcs and avoids spattering. Finally, it is possible to select the best combination of waveform and electrode-negative time for the application, using the equations presented to predict the weld bead geometry.

Introduction

The alternating current gas metal arc (AC GMA) process is also known as variable polarity gas metal arc welding (VP-GMAW), where the term "variable polarity" is more exactly used to describe waveforms in which the ratio of the two polarities can vary (Ref. 4). Yet the term AC is normally used to describe a sine wave, although it can also be used to describe a current that alternates between positive and negative polarities.

The VP-GMAW process combines the advantages of conventional GMAW (direct current electrode positive (DCEP)) with the increase in the melting rate of the wire and the reduction of thermal contribution when the GMAW process is operated with the electrode in the negative polarity mode (direct current electrode negative (DCEN)) (Refs. 5, 8). Therefore, it is possible to summarize the characteristics of the arc at both polarities as follows:

DCEP

- Electron flow from the workpiece to the electrode wire;
- Lower melting efficiency; and
- Most of the heat concentrated in the base material.

DCEN

- Electron flow from the electrodewire to the workpiece;
- Higher melting efficiency; and
- Most of the heat concentrated in the electrode.

Negative or combination polarities have been successfully used in processes that utilize fluxes such as brazing, flux cored arc welding, and submerged arc welding. The use of negative polarity (DCEN) to control the thermal contribution on the base metal and penetration in these processes have generated similar interest in GMAW. However, an obstacle that has limited the use of DCEN and variable polarity (or AC) in this process is the instability problem of the arc that comes with the use of negative polarity.

This problem is readily solved with the addition of stabilizing elements in processes that utilize fluxes. Instability problems in solid wire (GMAW) are more difficult to solve than the fluxed processes, which is why the welding with solid wire is operated almost exclusively with positive polarity. Direct current electrode negative polarity is usually limited to globular transfer, and it is seldom used because the resulting arc is unsteady and has an unacceptable spattering level (Refs. 9–11).

Most problems inherent to the DCEN use in GMAW are due to the strong repulsive force that acts under the droplet at the electrode wire tip (cathode). Since the electron flow is from the electrode wire toward the workpiece, repulsive force acting under the droplet appears due to electron emission, generating an erratic cathodic root and therefore an asymmetrically repelled droplet (Ref. 6).

The electrode activation has been employed to improve the electrons emission efficiency and to stabilize the cathodic points in DCEN. This is achieved through the addition of alkaline and rare-earth metals on the wire, but that is an expensive and not very popular method (Ref. 3). The use of blended shielding gases (Ar and O_2 and/or CO_2) has been reported as useful in the success of arc operation in DCEN. This is usually possible only at relatively high currents.

In order to overcome the reignition problems of the arc when the current

KEYWORDS

Variable Polarity
Alternating Current
Pulsed Current
Negative Electrode

L. O. VILARINHO (vilainho@mecanica.ufu.br), *A. S. NASCIMENTO, and D. B. FERNANDES are with Federal University of Uberlandia, Laprosolda (Center for R&D of Welding Processes), Uberlandia/MG, Brazil. C. A. M. MOTA is with Federal University of Para, Belem, PA, Brazil.*

passes through zero during the polarity change in AC, high voltage peaks are applied to keep the ionization of the arc column. However, the high voltage has always been a safety issue (Ref. 6). According to Harwig (Ref. 4), the voltage values applied when the current goes through zero depend on the amount of carbon dioxide in the shielding gas, and it can exceed 400 V.

With the advance of electronic technology, solutions for the past AC problems were found. The technology of inverters has made it possible and inexpensive to produce sources capable of generating almost all the conceivable waveforms (Ref. 3). Problems such as arc reignition when the current goes through zero are easily eliminated by the use of a rectangular waveform, which reduces the amount of time in which the current remains at or near zero (Ref. 3). This advantage eliminates the need for risky high voltages necessary to avoid the reignition problems with sine waveforms.

Characteristics such as low heat input, control over the bead geometry, low deformation, and higher melting rate compared to DCEP have called the attention of the industry, especially the automotive sector. Nevertheless, there is still little technical and scientific literature on the subject (Refs. 3–7), which contributes to the process' low popularity. In addition to that, the difficulty in determining parameters that provide good arc and metal transfer stability further discourage investments in VP-GMAW. Therefore, in this work, a methodology was developed to determine parameters in VP-GMAW for four different waveforms and variable negative-electrode rate at three levels. Looking for the effects of the welding parameters on the process operational performance and the weld metal quality, it is expected to contribute to the development of knowledge and optimization of the VP-GMAW application, promoting its popularization in different industrial segments.

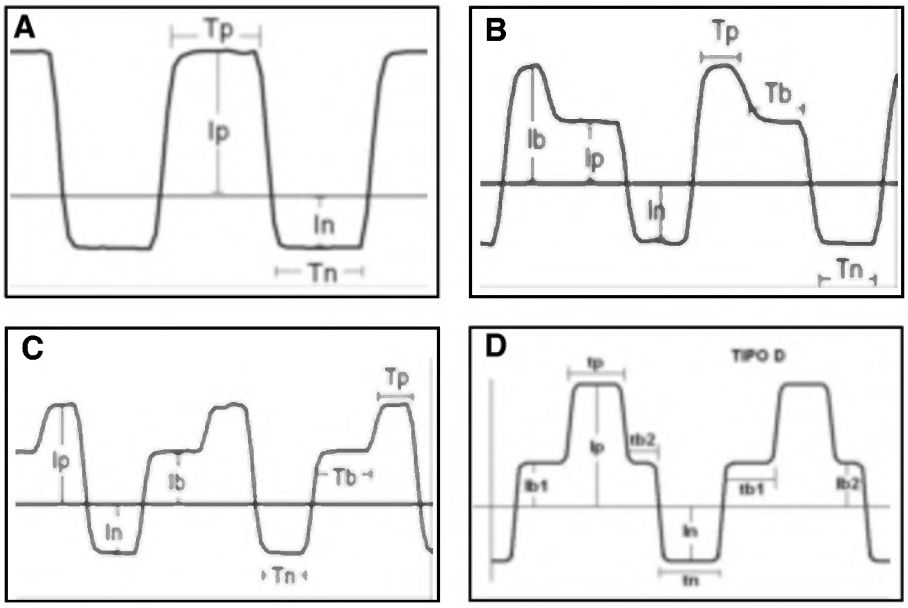

Fig. 1 — Studied waveforms. A — Type A; B — type B; C — type C; and D — type D.

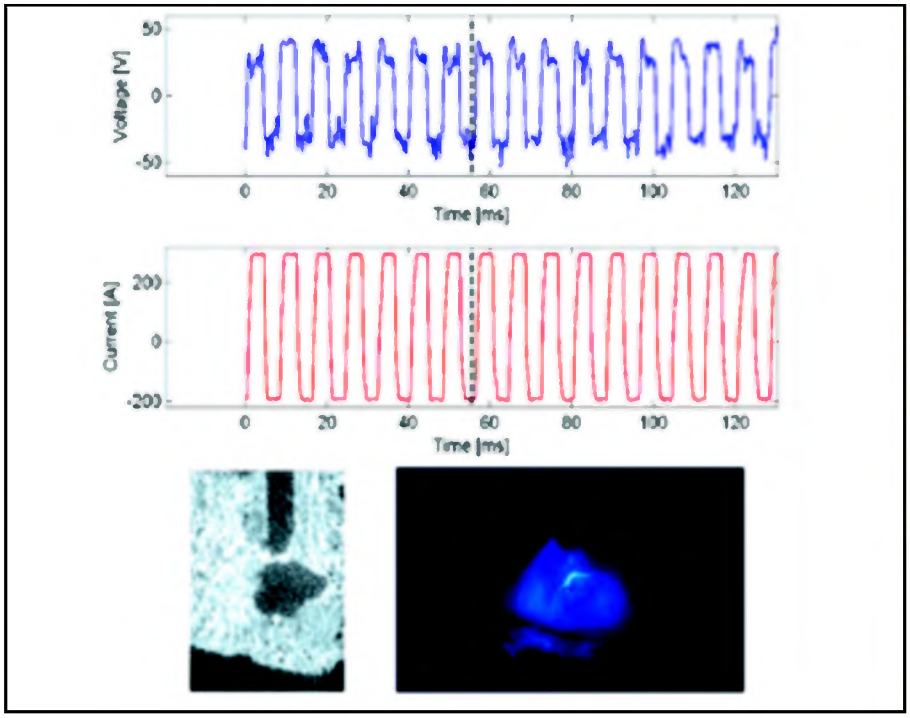

Fig. 2 — Synchronized high-speed images for waveform A and 50 %EN.

Experimental Procedure

In this work, a study was made focusing on the main parameters used in the VP-GMAW process to define a methodology that allows determination of such parameters in order to obtain both arc and metal transfer stability. In addition, an evaluation of the effect of the waveform and the negative polarity (%EN) on the geometrical features of the welding bead was made as well. Therefore, for a better understanding, the work will be divided in the three steps further described.

The experimental procedure consists of bead-on-plate weldments carried out on mild steel coupons (250 × 37 × 6 mm), with AWS ER70S-6 wire, 1.2 mm diameter, using Ar+2%O_2 as shielding gas at 15 L/min. A secondary-chopped power source was used as well as software/hardware for controlling it. This allows drawing of any waveform shape. For the workpiece displacement, an automatic XY coordinated table was used. The torch was at a fixed position to allow high-speed visualization of the metal transfer by backlighting the electrode wire. In this case, two high-speed filming cameras were employed, both synchronized between themselves and with the electrical signals (current and voltage) (Ref. 12), which were acquired by a DAQ system at 10 kHz and 16 bits.

Step 1: Determination of the Consumption Equation in the Positive and Negative Polarities

The equation of the melt-off rate (Ref. 13) WFS = $\alpha I_m + \beta L I_{ef}^2$ is a function of

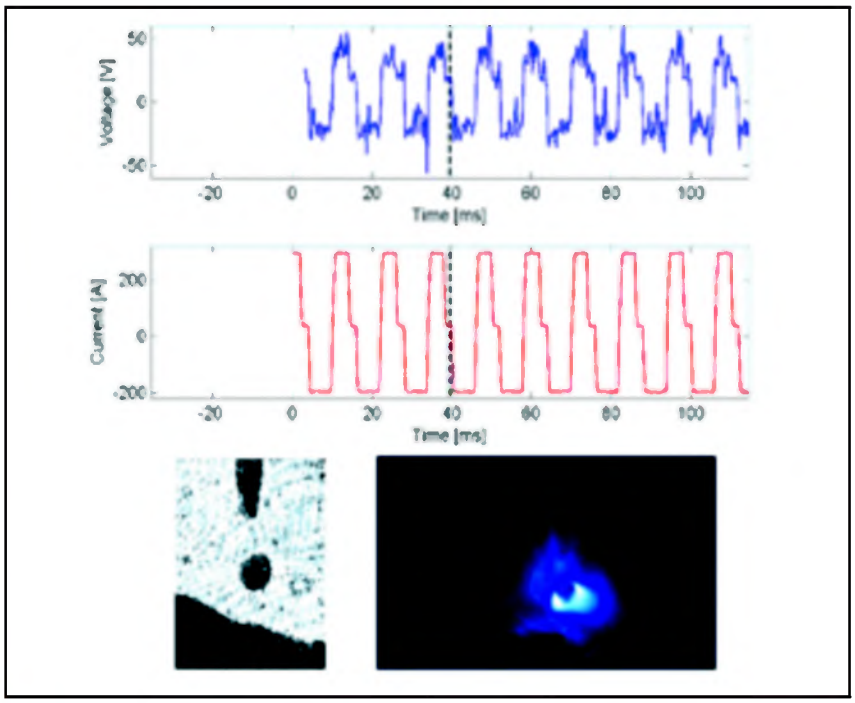

Fig. 3 — Synchronized high-speed images for waveform B and 50 %EN.

the constants α and β, which results in nonlinear parameter estimate (nonlinear regression), starting from the experimental determination of the other terms of the equation, where WFS is the wire feed speed, I_m is the mean current, L is the electrode extension, and I_{ef} is the RMS current.

The knowledge of the consumption equation in both polarities is fundamental to avoid the variation of arc length that occurs during the polarity change and, consequently, arc instabilities. Therefore, experiments were made in the positive as well as in the negative polarity where wire feed speed varied, keeping the arc length constant and the resulting values of medium current (I_m) and efficient current (I_{ef}), were then registered. With the data obtained experimentally, a nonlinear regression was carried out to determine the values of the constants α and β.

Step 2: Determination of Parameters that Guarantee Arc Length Stability

One of the main issues that generate instabilities in VP-GMAW is the arc length variation that occurs with the polarity inversion, since the melt-off rate in the negative polarity (DCEN) is greater than in the positive polarity (DCEP). Therefore, in order to obtain a constant arc length, a methodology was created for the determination of parameters based on the premise that the melt-off rate in the positive polarity be equal in the negative polarity, which is why it is so important to have knowledge of the melt-off rate equation.

This is a crucial point of the proposed methodology. The premise of making both positive and negative polarities equal always guarantees both arc stability and bead uniformity. However, stable condition sometimes can be reached at different melt-off rates. It means that the proposed methodology brings robustness to the welding process, which is the first step for its effectively industrial implementation.

Table 1 — Experimental Results in DCEP

Im(A)	Ief (A)	WFS (m/s)	L (m)
139	139	0.0500	0.015
171	171	0.0667	0.015
170	170	0.0667	0.015
194	194	0.0833	0.015
194	194	0.0833	0.015
218	218	0.1000	0.015
242	242	0.1167	0.015
282	282	0.1333	0.015

Im: mean current; Ief: RMS current; WFS: wire feed speed; and L: electrode extension.

Table 2 — Experimental Results in DCEN

I_m (A)	I_{ef} (A)	WFS (m/s)	L (m)
69	69	0.0500	0.015
117	117	0.0833	0.015
154	154	0.1167	0.012
200	201	0.1500	0.012
198	200	0.1500	0.012
241	246	0.1833	0.012
318	329	0.2167	0.012
297	332	0.2500	0.012

I_m: mean current; I_{ef}: RMS current; WFS: wire feed speed; and L: electrode extension.

Table 3 — Calculated Parameters for the Waveform A

Waveform A	I_p (A)	t_p (ms)	I_n (A)	t_n (ms)	%EN
	300	4	198	1.7	0.30
	300	4	198	4.0	0.50
	300	4	198	9.3	0.70

I_p: pulse current; t_p: pulse time; I_n: current; t_n: time at negative polarity; and %EN: percentage of electrode at negative polarity.

Table 4 — Calculated Parameters for the Waveform B

Waveform B	I_p (A)	t_p (ms)	I_n (A)	t_n (ms)	I_b (A)	t_b (ms)	%EN
	300	4	198	2.6	40	2	0.30
	300	4	198	6.0	40	2	0.50
	300	4	198	14.0	40	2	0.70

I_p: pulse current; t_p: pulse time; I_n: current; t_n: time at negative polarity; and %EN: percentage of electrode at negative polarity.

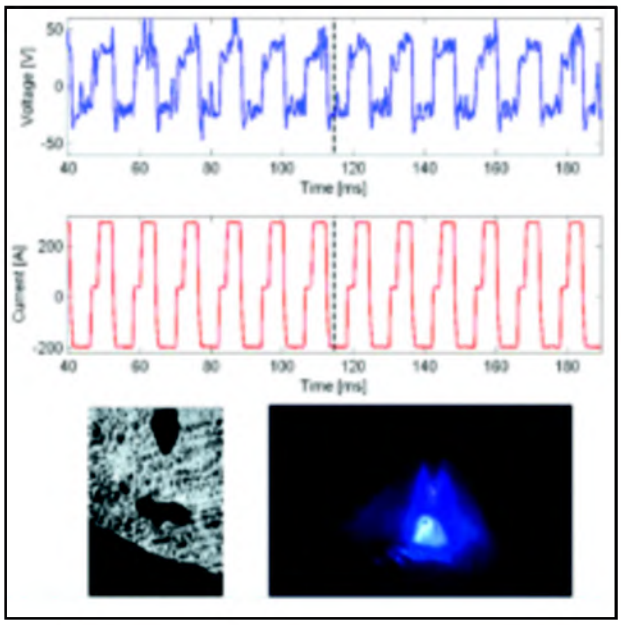

Fig. 4 — Synchronized high-speed images for waveform C and 50%EN.

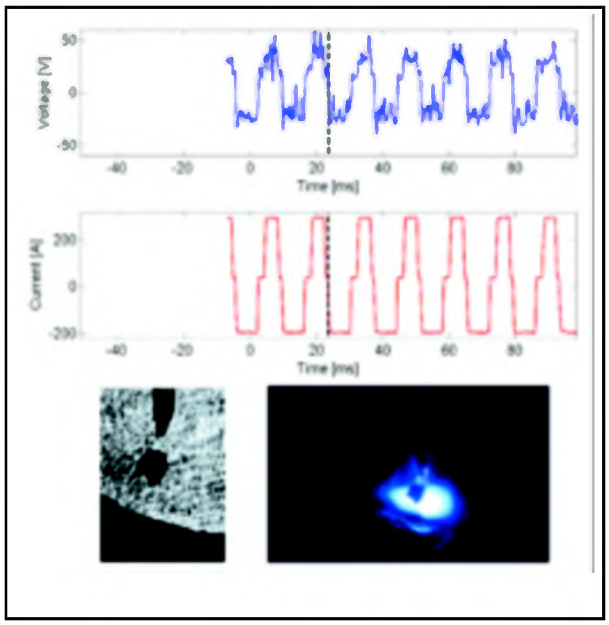

Fig. 5 — Synchronized high-speed images for waveform D and 50 %EN.

The base metal, welding wire, and shielding gas were the same as in the previous step, but now two fundamental parameters are analyzed in VP-GMAW:

- Waveform. Four different waveforms found in the literature (Refs. 4, 14) were evaluated, as shown in Fig. 1, in order to verify the effect of the sudden polarity change on the arc stability.
- EN rate. Three negative electrode percentage levels were evaluated (30, 50, and 70%) to verify their effects on the metal transfer. The %EN is defined by the ratio between the time length in which the electrode operates in the negative polarity and the period of time (time length in the negative plus the time length in the positive), as shown in Equation 1.

$$\%EN = \frac{t_{EN}}{t_{EN} + t_{EP}} \qquad (1)$$

where t_{EN} is the time at negative polarity and t_{EP} is the time at positive polarity.

With the influence factors defined, a calculation strategy was set to determine the parameters that guarantee both arc and metal transfer stability at a constant arc length.

Calculation strategy:

- Define pulse current (I_p) and pulse time (t_p) that guarantee one drop per pulse (ODPP);
- Define base current (I_b) obeying the arc stability criterion (Ib > 20A) (Ref. 2);
- Define base time (t_b) according to required %EN;
- Calculate negative current (I_n) for the waveforms, equalizing the melt-off rates at both polarities (WFS+ = WFS–);
- Calculate time in the negative (t_n) for the levels of %EN required, through Equation 2:

$$t_N = \frac{\%EN \cdot t_P}{(1 - \%EN)} \qquad (2)$$

where t_P = total positive polarity time.

Step 3: Evaluation of the Influence of Waveforms and %EN on the Bead Geometrical Features

With the parameters obtained in Step 2, bead-on-plate weldments were carried out in plain position, keeping the ratio between the wire feed speed and the welding speed (WFS/WS) constant. The bead features (depth, width, and reinforcement) and its superficial aspect as well as the spattering level were evaluated by visual inspection.

Results and Discussion

Results from Step 1: Determination of the Consumption Equations in the Positive and Negative Polarities

Tables 1 and 2 present the experimental results of the average and RMS currents for the negative and positive polarities, respectively.

The values calculated for α and β for the two polarities were, in the positive polarity case (DCEP) $\alpha = 2.74 \times 10^{-4}$ m/(s.A) and $\beta = 5.1 \times 10^{-5}$ s^{-1} A^{-2}, which are coherent with literature (Ref. 15) ($\alpha = 3 \times 10^{-4}$ m/(s.A) and $\beta = 5 \times 10^{-5}$ (s^{-1} A^{-2})). In the negative polarity case (DCEN), the values calculated were $\alpha = 7.14 \times 10^{-4}$ m/(s.A) and $\beta = 1.2 \times 10^{-5}$ s^{-1} A^{-2}. It is necessary to point out that in the positive polarity case both constants had statistical significance for 95% confidence. However, in the negative polarity case, only the α constant presented statistical significance for that confidence interval. Since the main heat-generating mechanism happens in the cathodic region, the results came to confirm this statement, because the α constant refers to that heat generation, while the β constant relates to the Joule effect, which starts to have a lesser effect in the case of DCEN, since lower current level is necessary for the same melt-off rate in DCEP.

Results from Step 2: Determination of Parameters that Guarantee Arc Length Stability

Following the calculation strategy, the current and pulse time were chosen based on a previous study (Refs. 1, 2) and were $I_p = 300$ A $t_p = 4$ ms. According to the arc stability criterion, the chosen base current was $I_b = 40$ A. The base times were $t_{b1} = 2$ ms and $t_{b2} = 1$ ms.

The value of negative current is calculated based on the chosen Ip, which is substituted in the equation of melt-off rate for DCEP. The resulting wire feed speed value is used in the melt-off rate equation for DCEN, and finally obtain the negative current to guarantee constant arc length (In = 198 A). Tables 3–6 present the pa-

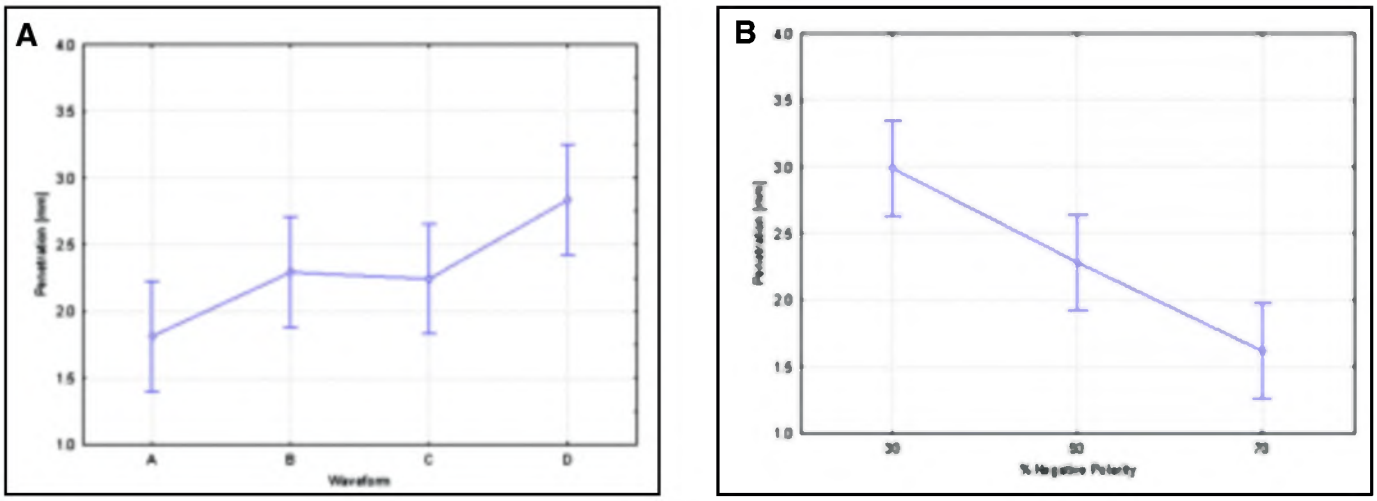

Fig. 6 — Effect of the waveforms (left, with p = 0.02915) and percentage of time at negative polarity (right, with p = 0.00172) on the penetration (for the whole model p = 0.003981). Vertical bars denote 0.95 confidence intervals.

Table 5 — Calculated parameters for the Waveform C

Waveform C	I_p (A)	t_p (ms)	I_n (A)	t_n (ms)	I_b (A)	t_b (ms)	%EN
	300	4	198	2.6	40	2	0.30
	300	4	198	6.0	40	2	0.50
	300	4	198	14.0	40	2	0.70

I_p: pulse current; t_p: pulse time; I_n: current; t_n: time at negative polarity; and %EN: percentage of electrode at negative polarity.

Table 6 — Calculated Parameters for the Waveform D

Waveform D	I_p (A)	t_p (ms)	I_n (A)	t_n (ms)	I_{b1} (A)	t_{b1} (ms)	I_{b2} (A)	t_{b2} (ms)	%EN
	300	4	198	3.0	40	2	40	1	0.30
	300	4	198	7.0	40	2	40	1	0.50
	300	4	198	16.3	40	2	40	1	0.70

I_p: pulse current; t_p: pulse time; I_n: current; t_n: time at negative polarity; and %EN: percentage of electrode at negative polarity.

rameters calculated for the studied waveforms and negative-electrode rate.

Through the analysis of the filming records and the weld coupons, it is possible to state that the highest level (70%) of the negative-electrode rate (%EN) presented the highest metal transfer instability for all waveforms. The droplets were usually three times as large as the electrode diameter and with an unacceptable amount of spatter, due to the intensified action of the repulsive force that actuates over the droplet when in DCEN. In addition, the excessive spatter accumulated within the nozzle, reducing the area of passage of the shielding gas, which caused interruptions of the arc and even the dislocation of droplets onto the nozzle border.

It was not possible to achieve the ODPP condition in the welding made with waveform A, without positive base current to "smooth" the polarity inversion. The drop detachments happened in an irregular and unstable way, with large drops and a large amount of spattering for all the %EN levels.

As for waveforms B–D, at the %EN levels of 30 and 50%, it was possible to achieve the ODPP condition, with drops of the same diameter as the wire. However, the waveform B presented beads with higher lateral spattering level, due to the fact that the base current in the positive polarity, which aims to "smooth" the current inversion, happens after the droplet transfer had occurred.

Figures 2–5 present results from the synchronization of the two high-speed cameras synchronized with current signal and voltage. The four figures refer to the %EN level of 50%. Figure 2 is related to waveform A and 50 %EN, and it can be noticed that the detached droplet has a much larger diameter than the electrode, due to the repulsive forces that retard the detachment; besides the detachment occurred in the negative polarity but not regularly.

The metal transfer in the waveforms B and C occurs regularly, always in the positive cycle, and it is stable. However, as can be observed in Fig. 4, the detachment of waveform C occurs at the end of the positive pulse and the droplet suffers action of repulsive forces that happen in the negative polarity. This decelerates the droplet, reducing its momentum, which allows it to be transferred more "gently" and reduces spattering. This phenomenon does not occur in waveform B, observed in Fig. 3, where the droplet is transferred quicker to the molten pool and always during the positive period. Therefore, because of the greater momentum, it causes more disturbance in the molten pool and, consequently, more spatter.

Finally, Fig. 5 represents the waveform D for 50% of %EN. In this condition, the metal transfer is very stable, since the change in polarity is not so sudden, due to the positive base before and

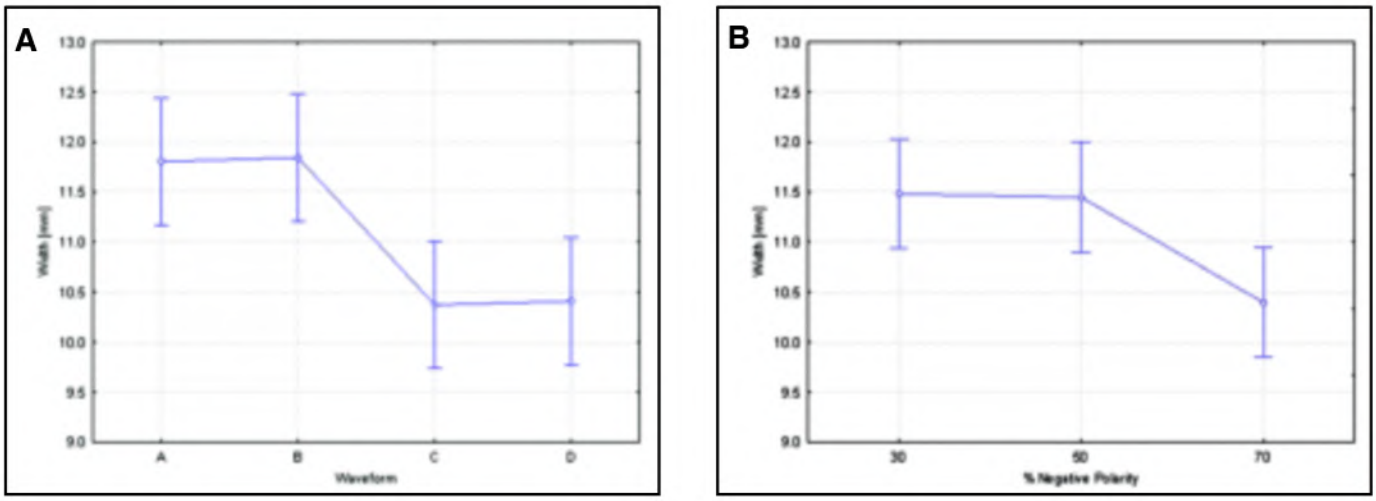

Fig. 7 — Effect of the waveforms (left, with p = 0.00917) and percentage of time at negative polarity (right, with p = 0.02347) on the bead width (for the whole model p = 0.009120). Vertical bars denote 0.95 confidence intervals.

after the detachment pulse.

Results from Step 3: Evaluation of the Influence of Waveforms and %EN on the Bead Geometrical Features

Table 7 presents the results of the geometrical characteristics of the beads in function of the waveform and negative-electrode rate (%EN). It also shows the coded variables for statistical analysis with the purpose of creating mathematical meta-models.

Figures 6–8 present the penetration, width, and reinforcement variation, respectively, as a function of the waveform (A, B, C, and D) and negative-electrode rate levels (%EN).

It is possible to perceive through the analysis of Fig. 6 that there is a clear tendency to reduction of penetration with the increase of the %EN for all four waveforms. This fact occurs because the %EN increase represents a longer negative polarity time and in that condition the heat is more concentrated in the electrode. Consequently, less thermal contribution in the base metal represents less penetration. Ueyama et al. (Ref. 8) found in their analyses on aluminum that by using 40 %EN the thermal contribution diminished and the maximum temperature on the plate was 140°C lower than in pulsed DC welding.

The same argument is used to explain the tendency of width reduction observed in Fig. 7, mainly for the 50 to 70%EN variation. Because the lower heat input, which occurs with the increase of the %EN, makes the wetting and melting of the base metal more difficult. Hence, the molten metal tends to concentrate on the surface of the pool increasing the reinforcement with the %EN increase, observed in Fig. 8.

On the other hand, waveform D at 70%EN did not follow this trend and experienced a smaller reinforcement value. This fact occurred due to the great instability generated by the high values of negative-electrode time, which intensified the repulsive forces on the droplet, which generated a loss of material due to spattering.

Mathematical models confirmed that could represent the behavior of the geometrical characteristics of the bead in function of the waveform and the negative-electrode rate (%EN). Two approximation models were tested and are represented by Equations 3 and 4:

$$y = A_0 + A_1p_1 + A_2p_2 \quad (3)$$

$$y = A_0 + A_1p_1 + A_2p_2 + A_3p_1p_2 \quad (4)$$

where A_0, A_1, A_2, and A_3 are constants; p_1 and p_2 are the parameters of influence (waveform and %EN, respectively); and y the response variable (penetration, width, or reinforcement).

For all the response variables, the average quadratic error, which considers the interaction of factors, was smaller for the first model (Equation 3) than for the second approximation model (Equation 4). This is the reason why a hypothesis test was made comparing the two models. Therefore, the best model for the response variable y is the one of Equation 3.

Equations 5–7 represent, respectively, the models resulting for penetration, width, and reinforcement in function of the waveform and %EN. It should be pointed out that the levels of the variables were coded, and they are shown in Table 7. These equations can be used for a technological point of view for predicting the weld bead geometry.

Table 7 — Results for Geometrical Features

Waveform Type	Coded	%EN Value	Coded	P (mm)	W (mm)	R (mm)
A	1	30	–1	2,41	12,43	3,48
A	1	50	0	1,58	12,56	3,56
A	1	70	1	1,45	10,42	4,27
B	2	30	–1	2,76	12,07	4,3
B	2	50	0	2,3	12,26	4,7
B	2	70	1	1,82	11,2	4,9
C	3	30	–1	2,98	10,92	4,47
C	3	50	0	2,45	10,28	4,88
C	3	70	1	1,3	9,92	4,89
D	4	30	–1	3,8	10,5	4,9
D	4	50	0	2,8	10,68	5,16
D	4	70	1	1,9	10,05	4,63

Weld bead dimensions: P = penetration, W = width, and R = reinforcement.

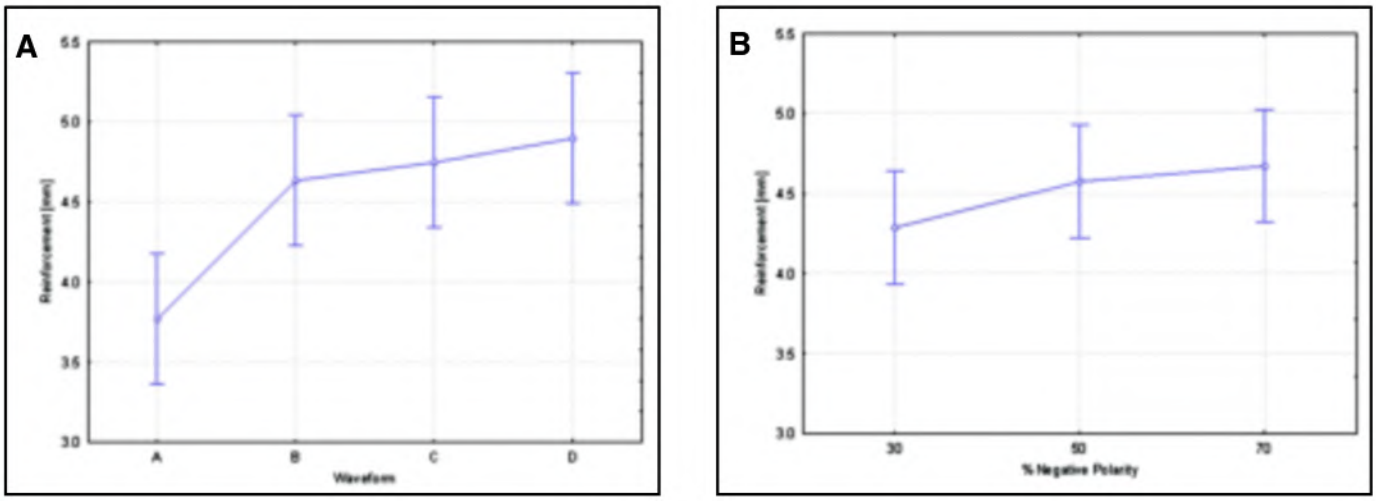

Fig. 8 — Effect of the waveforms (left, with p = 0.01151) and percentage of time at negative polarity (right, with p = 0.22611) on the reinforcement (for the whole model p = 0.022157). Vertical bars denote 0.95 confidence intervals.

$$P = 1.5433 + 0.3WF - 0.685EN \quad (5)$$

$$W = 12.52 - 0.565WF - 0.541EN \quad (6)$$

$$R = 3.6383 + 0.349WF + 0.1925EN \quad (7)$$

where P is the penetration, W is the width, R is the reinforcement, WF is the waveform, and EN is the %EN.

Conclusions

In general terms, it is possible to conclude that the proposed methodology for parameter calculation successfully accomplished the task of reaching both arc and metal transfer stability. More specifically, it can be conclude that

- The knowledge of the melt-off rate equation in the negative and positive polarities is fundamental to determine parameters in VP-GMAW that provide a more stable arc with constant length;
- The positive base before and after the pulse (waveform D) is beneficial in reducing abrupt polarity changes, but, for higher %EN, long negative time always generates great instability;
- Waveforms B and C provide arcs that are stable and with ODPP. However, the base before the pulse (waveform C) is more effective in avoiding spattering;
- There is a reduction in the penetration with the increase of the %EN due to the reduction of the thermal contribution, which allows thin-plate welding and linings application;
- It is possible to select the combination of waveform and %EN more adequately depending on the application, using the equations presented to predict the weld bead geometry.

Acknowledgments

The authors wish to thank the Brazilian agency Fapemig under grant TEC APQ 3287-6, the CNPq council, IFM, and UFU for financial support.

References

1. Vilarinho, L. O., Balsamo, S. S., and Scotti, A. 2000. Nonlinear synergic command for pulsed MIG equipment with constant current (in Portuguese). Instituto Nacional da Propiedade Industrial, Patent BR-200006339 A: Brazil.

2. Vilarinho, L. O., and Scotti, A. 2000. An alternative algorithm for synergic pulsed GMAW of aluminum. *Australasian Welding Journal* 45(2): 36–44.

3. Harada, S., et al. 1999. The state-of-the-art of AC-GMAW process in Japan. IIW Doc. XIII-1589-99, p. 10.

4. Harwig, D. D. 2003. Arc behaviour and melting rate in the VP-GMAW process. PhD thesis, Cranfield University: UK. p. 221.

5. Mulligan, S. J. 2003. Pulsed MIG arc welding processes for joining of thin sheet aluminium. Doc. 771/2003, The Welding Institute.

6. Talkington, J. E. 1998. Variable polarity gas metal arc welding. The Ohio State University, p. 126.

7. Harwig, D. D. et al. 2006. Arc behavior and melting rate in VP-GMAW process. *Welding Journal* 85(3): 52s to 62s.

8. Ueyama, T., et al. 2005. AC pulsed GMAW improves sheet metal joining. *Welding Journal* 84(2): 40–46.

9. Lucas, W., Iordachescu, D., and Ponomarev, V. 2005. Classification of metal transfer modes in GMAW. IIW Doc. No XII-1859-05, p. 9.

10. Vilarinho, L. O. 2007. Fundamental modes of metal transfer: Natural and controlled (in Portuguese). *Revista da Soldagem* Maio: 14–19.

11. Iordachescu, D., Lucas, W., and Ponomarev, V. 2006. Reviewing the "Classification of Metal Transfer." IIW Doc. No. XII-1888-06, p. 10.

12. Balsamo, S. S., Vilarinho, L. O., and Scotti, A. 2000. Development of an experimental technique for studying metal transfer in welding: Synchronized shadowgraphy. *Int. J. for the Joining of Materials* 12(1): 48–59.

13. Lesnewich, A. 1958. Control of melting rate and metal transfer in gas-shielded metal-arc welding: Part 1 - control of electrode melting rate. *Welding Journal* 37(8): 343s to 353s.

14. Farias, J. F., et al. 2005. Effect of the alternating current MIG/MAG welding on the weld geometry (in Portuguese). *Soldagem & Inspecao* 10(4): 173–181.

15. Norrish, J. 1992. Advanced welding process. Institute of Physics Publishing, Bristol, Philadelphia, and New York. p. 375.